

EFFECT OF THE GROWTH TIME ON THE OPTICAL PROPERTIES OF ZnO NANORODS GROWN BY LOW TEMPERATURE METHOD

A. F. ABDULRAHMAN^{a*}, S. M. AHMED^b, M. A. ALMESSIERE^c

^a*Department of Physics, Faculty of Science, University of Zakho, Zakho,
Kurdistan Region, Iraq*

^b*Department of Physics, College of Science, University of Duhok, Duhok,
Kurdistan Region, Iraq*

^c*Physics Department, Collage of Science, University of Dammam, Dammam,
Kingdom of Saudi Arabia*

ZnO nanorods have been synthesized on glass substrate by low-cost two step chemical bath deposition (CBD) method at low temperature. The ZnO seed layers have been coated on glass substrate by RF magnetron techniques with power 150 watt for 15 min. The influence of different growth time on the optical properties, energy band gap, Raman spectra and surface morphology of ZnO nanorods are investigated. The growth time are (0.5, 1, 2, 3, 4 and 5) h. The double beam UV visible (UV-5000) , Raman Spectroscopy and field emission scanning electron microscopy have been used to characterize the optical properties (absorption and transmission), energy band gap, Raman spectra, surface morphology, diameter, distribution and homogeneity of produced ZnO nanorods. The results found that the growth time have significant effect on the optical properties, energy band gap, Raman modes, aligned, surface morphology, diameter, ZnO distribution and density. And It is observed that the absorbance of the growth times 4 and 5 h are higher than the other growth times of ZnO nanorods, which showed the good crystallinity of the other samples. The transmittance decreases sharply near UV region at wavelength around 385 nm due to the optical band gap absorption. The obtained energy band gap of ZnO nanorods decreases with increase in the growth time from 3.25 eV to 3.18 eV. From result, it was investigated that the growth time caused the average crystalline size increases and decreases defects causing the energy band gap decreased. From Raman spectra , it observed that the dominant and sharp peaks at approximately 100 cm⁻¹ and 437 cm⁻¹ for the ZnO nanorods grown of 4 h and 5 h as a growth times, which are corresponds to the intrinsic characteristics of the Raman active E_{2(low)} and E_{2(high)} modes of the hexagonal wurtzite ZnO, respectivlyAlso FESEM results shows that the growth time has a good playing role on the nanostructure growth orientation of the ZnO nanorods.

(Received July 25, 2017; Accepted October 12, 2017)

Keywords: ZnO Nanorods, Optical Properties, CBD, Growth Time.

1. Introduction

Recently, zinc oxide (ZnO) is one of the versatile n-type and technologically significant semiconducting material due its unique properties such as direct band gap (3.37 eV), transparency in the visible range, abundance in nature, absence of toxicity, high-electrochemical stability and resistivity control over range 10⁻³ to 10⁵ Ωcm [1]. ZnO has large direct band gap energy (3.37 eV) and wide exciton binding energy (60 meV) at room temperature, high mechanical, chemical and thermal stability, excellent optical and electrical properties and biocompatibility [2], which makes the material useful for optoelectronic devices such as, UV light sensors, gas sensors, dye sensitized solar cells, transparent conducting layers, photocatalysts, blocking layer in flexible organic solar cell, light emitting devices and thin film transistors [3-10]. ZnO nanostructures of such as ZnO nanorods, nanowires and nanotubes have received considerable attention due to their unique

*Corresponding author: ahmadamedi@yahoo.com

optical and electrical properties [11]. Due to the high surface to volume ratio provided by the one dimensional (1D) nanostructure, ZnO nanorod arrays are more appropriate to the implementation for crossbred photovoltaic devices [12]. ZnO nanorods have been fabricated by using different chemical and physical techniques such as chemical bath deposition [13], hydrothermal [14], RF sputtering [15], electrodeposition [16], spray pyrolysis [17], metal organic chemical vapor deposition [18], vapor phase transport [19], pulsed laser deposition [20], molecular beam epitaxy [21] and thermal evaporation [22]. Among these fabrication methods, chemical bath deposition also indicated to as solution deposition method and one of the more effective and efficient synthesis method for fabricating ZnO nanorods because it has own advantages such as reproducibility, simplicity, non-hazardous and low cost. The chemical bath deposition method is well suited for producing large area thin films. This method is low temperature method and it does not require sophisticated instruments. It involves deposition of semiconductor thin films on substrates that are kept in the aqueous solutions [23].

There are different growth parameters can effect on the fabrication of ZnO nanorods in the chemical bath depositions (CBD) methods such as, pH of growth solution, precursor concentration, bath temperature, thickness of the seed layer, type of substrates and growth time [24]. In the chemical bath deposition method, the growth time is the essential and significant growth parameters that directly effect on shape and size of ZnO nanorods [25]. The optical and structural properties of ZnO nanorods are significantly depend on the size, shape and morphology of one dimensional (1D) ZnO nanorods. Thus, thorough understanding of the effects of preparation parameters especially growth time on morphology of ZnO nanorods which control the growth mechanism of ZnO nanorods are considered essential [26]. In this paper, ZnO nanorods have been fabricated on glass substrates by using low-cost chemical bath deposition method at low temperature 95 °C. The influence of the growth time on the optical properties, energy band gap, Raman spectra, surface topography and growth process of the ZnO nanorods have been studied.

2. Experimental Details

All chemical materials that used in this study are of analytical grade from Sigma-Aldrich Company, and used as beginning materials without further purification. The experimental setup and the synthesis method have been described in our previous studies [27-28].

2.1 Preparation of Samples

The microscopic glass is utilized as substrates for growing ZnO nanorods. The glass substrates have been cleaned in an ultrasonic bath by using ethanol, acetone and deionized water for 15 min respectively and dried with nitrogen gas. A radio frequency (RF) magnetron sputtering was used to deposit the 100 nm thick ZnO seed layer on the cleaned glass substrates using target (99.999% purity of ZnO). The 100 nm thick ZnO seed layer was deposited on the glass substrates with 5.5×10^{-3} mbar argon gas pressure inside RF chamber and 150 Watt RF power sputtering for 15 min. After that the fabricated ZnO seed layer on glass substrates annealed inside tubular furnace at 400 °C for 2 h under atmosphere to stress relief the coated layer.

2.2 Growth Process

The low temperature method chemical bath deposition (CBD) method has been employed for fabrication vertically aligned ZnO nanorods on glass substrates for various growth times. The Zinc Nitrate Hexahydrate ($Zn(NO_3)_2 \cdot 6H_2O$) and Hexamethylenetetramine (HMTA) ($C_6H_{12}N_4$) are utilized as precursors, and deionized water was used as a solvent. The suitable amount of the Zinc Nitrate Hexahydrate equal molar concentration of the Hexamethylenetetramine were separately dissolved in deionized water at 80 °C and mixed together under magnetic stirrer. The prepared ZnO seed layer coated glass substrates were inserted vertically inside a beaker including a mixture of the two solutions. To investigate the effect of the different growth time on optical properties, energy band gap, Raman spectra, surface topography and growth of ZnO nanorods on glass substrates, beakers are placed inside an oven at 95 °C for various growth time (0.5, 1, 2, 3, 4 and 5) hrs. At the end of growth process the all samples were rinsed by deionized water to remove the

remaining salt, and then it was dried by nitrogen gas. The growth mechanism of the formation of ZnO nanorods can be shown on based of chemical reactions in chemical bath deposition (CBD) process can be summarized as below [29]:



2.3 Characterization Techniques

The optical properties (absorption and transmission) spectrum and energy band gap of the ZnO nanorods for different growth time were characterized at room temperature using the Cary 5000 UV-Vis-NIR Spectrophotometer with a wavelength range 300 nm to 800 nm. The Raman spectra of ZnO nanorods were collected at room temperature using Raman spectroscopy System model: HR 800 UV, HORIBA Jobin Yvon, and Edison. The surface morphology, diameter, length, distribution and density of ZnO nanorods for various growth time were examined using by Field Emission Scanning Electron Microscope (FESEM), the model of the FESEM is (FEI Nova a nano SEM 450 Netherlands and Leo-Supra 50 VP, Carl Zeiss, Germany).

3. Results and Discussion

The optical properties of ZnO nanorods grown on glass substrates using low temperature methods are investigated based on observation of the optical absorptions and transmissions through the ZnO nanorods films using UV-Vis spectrometers and it will be discuss. The optical absorption spectrum of the ZnO nanorods synthesis at the 95 °C for different growth time 0.5 h to 5 h with wavelength range between 300 nm to 800 nm as shown in figure 1. It can clearly seen that the absorbance spectrum reveals the strong absorption (high absorbance) in UV region at wavelength below 400 nm and high transparency (low absorbance) in visible region, which is the characteristics of ZnO [30]. The low absorption values at long wavelengths are related to the defects of the ZnO nanorods film such as oxygen vacancies and interstitial Zn atoms, which act as donor impurities [31]. The sharp UV absorption edge of the all the samples are found approximatly at wavelength of 385 nm, which is crosspounded to the optical energy band gap of the ZnO nanorods. As the growth time increases, the absorption edge shifted towards longer wavelength [32-34].

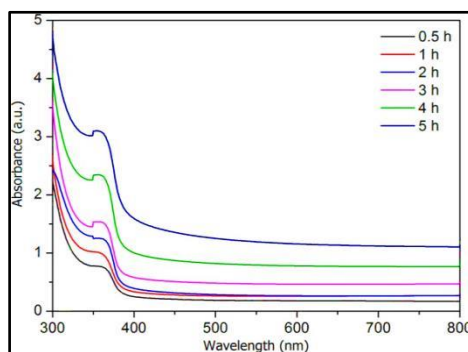


Fig. 1. Optical absorption spectrum of ZnO nanorods at 95 °C for different growth time

The shift of the absorption edge to higher wavelength was caused by the reduction of the transition distance between energy levels usually called band gap energy [32, 34]. The absorbance has increased with increases in the growth time [30, 15 and 36]. This may be due to increase in the hydroxide accumulation along grain boundaries and topographical changes of the ZnO nanorods after growth time increases [1]. Also it is observed that the absorbance of the growth times 4 and 5 h are higher than the other growth times of ZnO nanorods, which showed the good crystallinity of the other samples. And also have high internal surface area for electrolyte adsorption [30]. Fig. 2 shows the effect of the different growth time on the optical transmittance spectrum of ZnO nanorods fabricated at low temperature with wavelength range between 300 nm to 800 nm. It is investigated that most the ZnO nanorods samples in the visible region have high transmittance and low transmittance in the UV region. The higher transmittance is found for ZnO nanorods films grown for 0.5 h, which is decreases from (~70 %) to (~ 8 %) by increase in the growth time to 5 h [32- 34, 37-38] . This may basically be due to enhanced scattering effect in ZnO nanorods films grown at longer time [39].

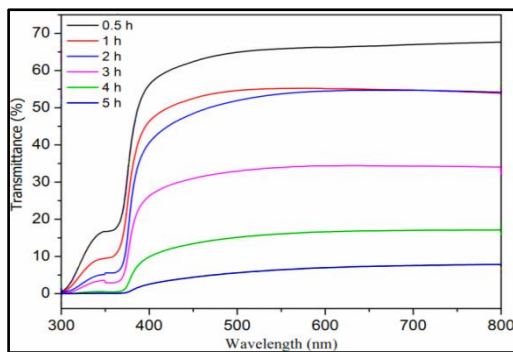


Fig. 2. Optical Transmission spectrum of ZnO nanorods at 95 °C for different growth time

The transmittance decreases sharply near UV region at wavelength around 385 nm due to the optical band gap absorption. At higher growth time (> 0.5 h), the ZnO nanorods thin films observe a reduction in the optical transmittance spectrum due to the scattering at the grain boundaries [40, 34]. The transmittance of the ZnO nanorods films increases when the crystallite size is smaller due to decreased optical scattering [41-44] In addition, the c-axis orientation also affects the transmittance of the produced films. The transmittance increases with the preferred c-axis orientation, which is consistent with a reduction in light dispersion at grain boundaries as the film structure becomes more oriented along the c-axis [45]. Moreover, the increase in film thickness at higher growth time increases the optical scattering, which reduces the transmittance of the thin films [33-34]. The transmission spectra are shifted to longer wavelength with growth time increases that means the optical properties of produced ZnO nanorods have been changed [32, 34]. The shift of the absorption edge to higher wavelength was caused by the reduction of the transition distance between energy levels usually called band gap energy [32], and may be attributed to the internal stress produced in the film and the light scattering effects in the films caused by the random distribution of the nanorod arrays [33]. In general, the surface roughness, defect centers and oxygen vacancies are three influence factors that effecting on the transmittance of ZnO nanorods thin films [46]. In this study, the decrease of transmittance of the produced ZnO nanorods thin films with increases the growth time could be concerned to the two factors. First, the thicker ZnO nanorods thin films with growth time increases had large hexagonal grain size and larger surface roughness. Second, is the thicker ZnO nanorod thin films result the higher absorption. The absorption coefficient can increase with the present of oxygen vacancies [34].

The optical energy band gap of ZnO nanorods fabricated at low cost CBD method is evaluated by the extrapolation of the linear portion of $(\alpha h\nu)^2$ versus $h\nu$ plots using Tauc formula [47]:

$$(\alpha h\nu)^2 = A(h\nu - E_g)^n \quad (6)$$

Where α is the absorption coefficient, $h\nu$ is the photon energy, A is constant, E_g is the optical energy band gap and n depends on the transmission type (equals to 1/2 for allowed direct transmission and 2 for indirect transition). It is known that the zinc oxide (ZnO) is direct transition semiconductor, then the value of n is 1/2.

The Tauc plot ($\alpha h\nu)^2$ versus energy band gap ($h\nu$) of the ZnO nanorods fabricated on glass substrates grown for various growth time is shown in figure 3. From the plots, it is observed that the transition region is around 3.2 eV, which is crosspounded to the direct transition band between the edges of valance and conduction band that represent the optical energy band gap of the ZnO semiconductor [30]. The obtained values of the direct energy band gap (E_g) of ZnO nanorods are 3.250 eV, 3.240 eV, 3.2334 eV, 3.230 eV, 3.221 eV and 3.170 eV grown for different growth time of 0.5 h, 1 h, 2 h, 3 h, 4 h and 5 h, respectively. The energy band gap of fabricated ZnO nanorods decreases with increasing growth time due to reduction of surface area [35, 38, 48-50]. And this decreases in energy band gap with increases the growth time also may due to the increasingly the crystalline size caused by the quantum size effect [51]. The obtained energy band gap results are in good agreement with other previous studied [52]. The energy band gap (E_g) is related to the grain size, carrier concentration and stress state in the material [53]. The maximum of energy band gap for the ZnO nanorods grown at 0.5 h as a growth time may be related to the smallest grain size. Furthermore, with increasing growth time, the decrease of energy band gap should be related to the increase of grain size, decrease of carrier concentration, and the tensile stress and oxygen vacancies which lead to the decrease of the carrier concentration in the conduction band [54]. On the other hand, it investigated that the growth time caused the average crystalline size increase and decreases defects causing the energy band gap decreases. Generally, the optical energy band gap of ZnO nanorods are lower rather than ZnO bulk and about 3.37 eV, this is due to the optical confinement effect of the formation of ZnO nanorods [55].

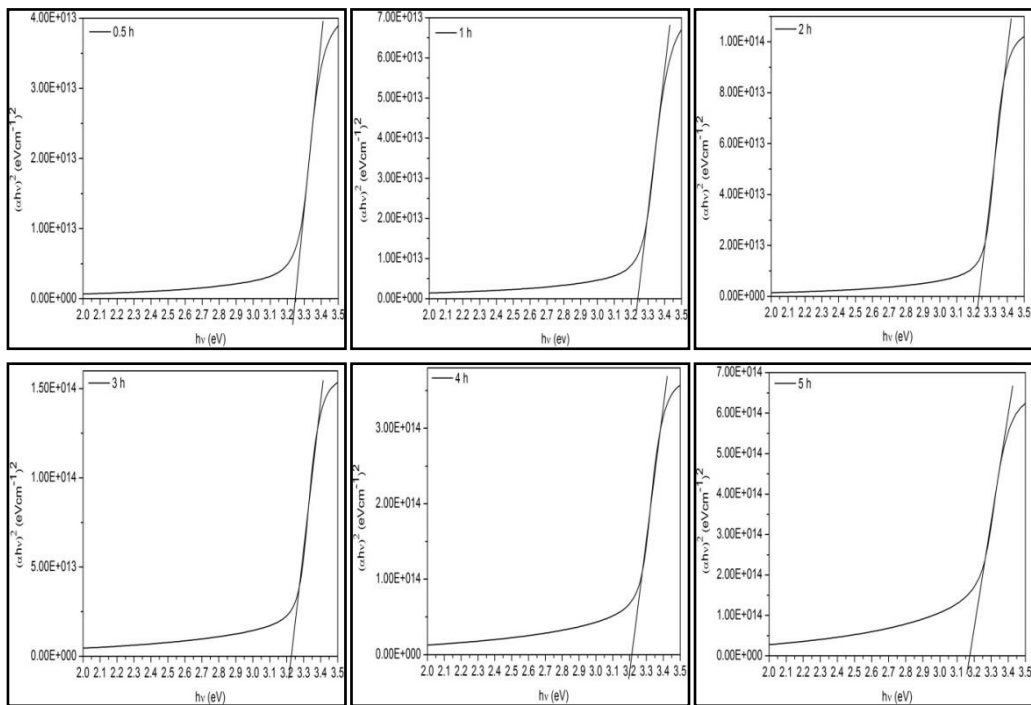


Fig. 3. The Tauc plot ($\alpha h\nu)^2$ versus energy band gap ($h\nu$) of the ZnO nanorods for different growth time

The micro-Raman scattering is one of the non-destructive and contactless studies and subsequently it does not need any special preparation of the sample for measurements. And it is an effective tool to examine (analyze) the phase orientation, quality of material, interaction of phonons and transport properties [56-57]. Wurtzite ZnO belongs to the space group of C_{6v}^4 which predicts that the eight sets of phonon modes are observable at wave vector $k \approx 0$ (Γ point). In the eight

phonon modes of ZnO, six of them are optical phonon modes and remaining two phonon modes are acoustic. According to group theory, the optical mode at the Γ point of the Brillouin zone can be represented by [57-59].

$$\Gamma = 1A_1 + 2B_1 + 1E_1 + 2E_2 \quad (7)$$

Among these modes, the $1A_1$, $1E_1$ and $2E_2$ modes are Raman active. The A_1 and E_1 modes are infrared active and only E_2 mode is Raman Active. The $2B_1$ modes are silent modes. Both A_1 and E_1 modes are split into transverse optical (TO) and longitudinal optical (LO) phonons. Non-polar phonon modes with E_2 symmetry separate into two frequencies; $E_{2(\text{high})}$ modes are associated with oxygen atoms and $E_{2(\text{low})}$ modes are associated with Zn sublattice. Because the Raman scattering is perpendicular to the c-axis of ZnO nanorods, so only $E_{2(\text{high})}$ and $A_{1(\text{LO})}$ are Raman active [57, 60]. Figure 4 shows the typical Raman spectra of ZnO nanorods grown on glass substrates at low temperature (95°C) for different growth time which are 0.5, 1, 2, 3, 4 and 5 h. The appearance of dominant and sharp peaks at approximately 100 cm^{-1} and 437 cm^{-1} for the ZnO nanorods grown of 4 h and 5 h as a growth times, which are corresponds to the intrinsic characteristics of the Raman active $E_{2(\text{low})}$ and $E_{2(\text{high})}$ modes of the hexagonal wurtzite ZnO, respectively. The existence of a sharp and dominant peak of $E_{2(\text{high})}$ mode without $E_{2(\text{low})}$ mode confirms that the grown ZnO nanorods have a hexagonal wurtzite structure with a good crystal quality [57, 61]. The weak peaks at approximately 332 cm^{-1} which is associated with $E_{2(\text{high})}$ - $E_{2(\text{low})}$ (multible phonon process), and the $A_{1(\text{TO})}$ mode is showed around 377 cm^{-1} are observed for the ZnO nanorods grown of 3 h, 4 h and 5 h as s growth time [62]. The peaks 480 cm^{-1} , 560 cm^{-1} and 580 cm^{-1} are corsepond to the $E_{1(\text{Low})}$ mode to impurities and structural defects (oxygen vacancies and Zn interstitials).

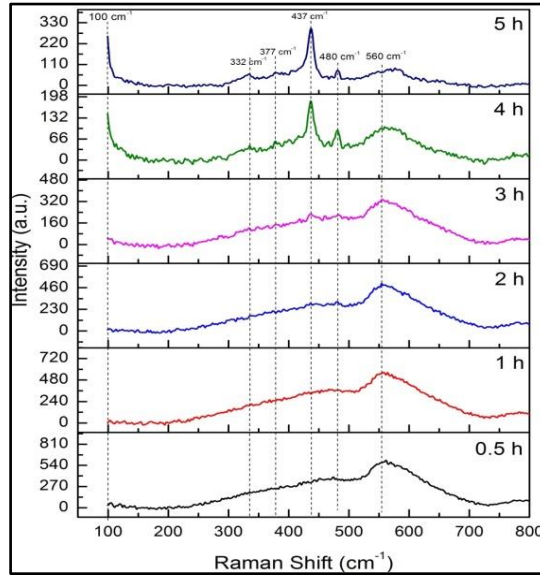


Fig. 4. Typical Raman spectra of ZnO nanorods grown on glass substrates for different growth time

The intensities of the $E_{1(\text{Low})}$ decreases with increase the growth time. The intensities of the ZnO Raman active peak become higher as the growth time increases, which indicate the increase in the crystal quality of the nanorods and/or the increase in the coverage of the nanorod arrays on the substrate [62]. The surface morphology, cross section, length, diameter, density and distribution of the ZnO nanorods fabricated using CBD method at low temperature for different growth time from 0.5 h to 5 h are shown in figure 5. From figure 5, the ZnO nanorods that grown of 0.5 h have nonhomogeneous distribution of the ZnO nanorods and low density all over the seed. Also the formation of the most of the ZnO nanorods look like a grain of rice comprises of single ZnO nanorods with the average length and average diameter are 255nm and 55 nm, respectively. As the growth time is increased to 1 h, the ZnO nanorods structure started to form. It was observed

that the ZnO nanorods were randomly oriented and not vertically aligned of ZnO nanorods with average diameter and average length are 62 nm and 493 nm, respectively, and more distribution over the seed. As the time of growth is increased to 2 hours, the formation of ZnO NRs occur more uniformly with higher distribution and density. The average diameters and average length of ZnO nanorods are increased to 67 nm and 683 nm, respectively [29]. However, the aligned of ZnO nanorods is still not good enough. Further increasing of growth time to 3 hours the average ZnO nanorods diameter and length was boosted to 91 nm and 1008 nm and 164 nm, 1068 nm for growth time 4 and 5 hours, respectively. From all images in figure 5, one can notice that the growth time is well important parameter in obtaining the morphology (density, size, shape, distribution, orientation and alignment) of the ZnO nanorods. Also one can notice from figure one that the diameters and shape of ZnO nanorods are completely depend on growth time [29].

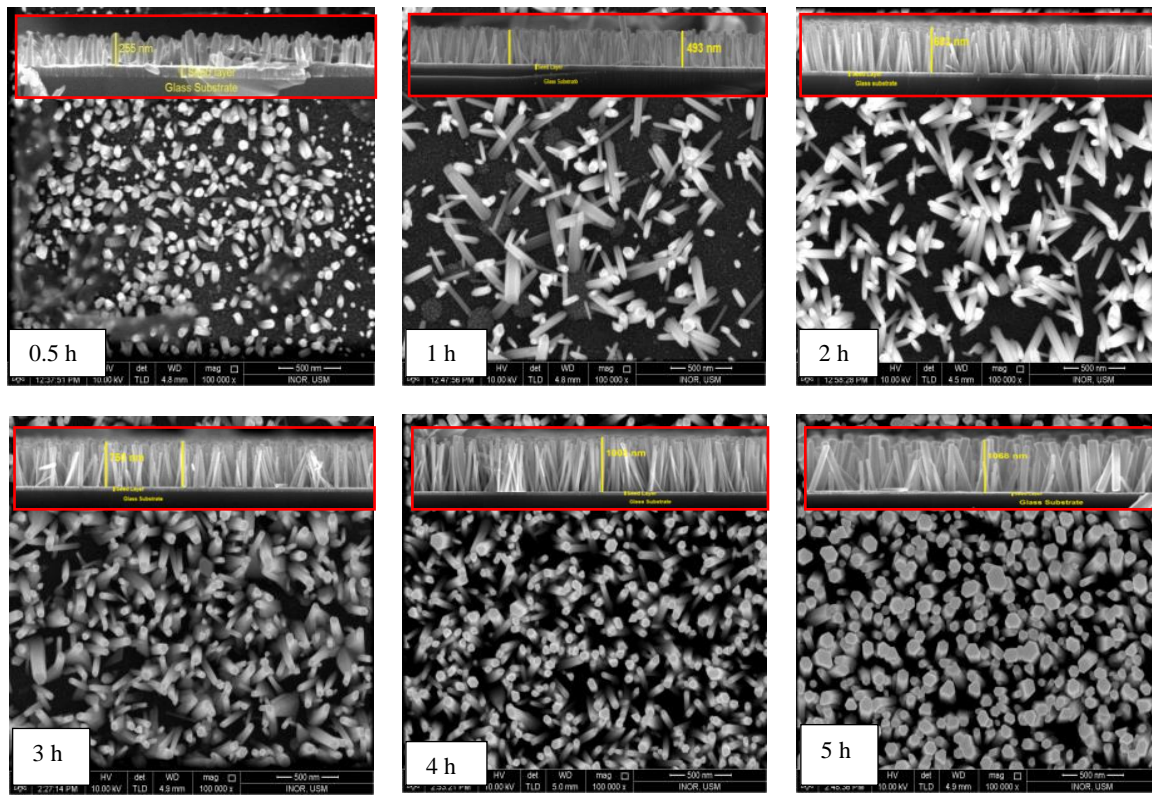


Fig. 5. (Top view & cross section) FESEM images of the ZnO nanorods grown on glass substrates at 95 °C for different growth time

4. Conclusions

Very high quality ZnO nanorods were successfully fabricated on ZnO/glass substrates by chemical bath deposition (CBD) method at 95 °C. The influence of the growth time on optical properties (absorption and transmittance), optical energy band gap, Raman spectra, cross section and surface morphology (length and diameter) of synthesized ZnO nanorods are studied. It was found that the absorbance has increased with increases in the growth time. The transmittance of the films increases when the crystallite size is smaller due to decreased optical scattering.. The intensities of the ZnO Raman active peak become higher as the growth time increases, which

indicate the increase in the crystal quality of the nanorods and/or the increase in the coverage of the nanorod arrays on the substrate. From FESEM, one can conclude that the growth time consider a very significant growth parameter for controlling the size, shape, distribution and alignment of ZnO nanorods. The average length and average diameter of the ZnO nanorods are increase with increasing the growth time.

References

- [1] V. R. Shinde, C. D. Lokhande, R. S. Mane, S. H. Han, *Applied Surface Science* **245**, 407 (2005).
- [2] O. Lupon, L. Chow, G. Chai, B. Roldan, A. Naitabdi, A. Schulte, H. Heinrich, *Materials Science and Engineering B* **145**, 576 (2007).
- [3] A.J. Gimenez, J.M. Yez-Limón, J.M. Seminario, *J. Phys. Chem. C* **115**(1), 282 (2011).
- [4] Ng. L. Hung, E. Ahn, H. Jung, H. Kim, D. Kim, J. Kor. Phys. Soc. **57**(6), 1784 (2010).
- [5] Q. Zhang, C.S. Dandeneau, X. Zhou, G. Cao, *Adv. Mater.* **21**(41), 4087 (2009).
- [6] M-J. Keum, B-J. Cho, H-W. Choi, S-J. Parka, K-H. Kim, *J. Ceram. Process. Res.* **8**(1), 56 (2007).
- [7] A. Lei, B. Qua, W. Zhou, Y. Wang, Q. Zhang, B. Zou, *Mater. Lett.* **66**, 72 (2012).
- [8] C.Y. Lee, M.Y. Lin, H.W. Wu, J.Y. Wang, Y. Chou, W.F. Su, Y.F. Chen, C.F. Lin, *Semicond. Science Technol.* **25**(10), 105008 (2010).
- [9] S.K. Jha, O. Kutsay, I. Bello, S.T. Lee, *J. Luminesc.* **133**, 222 (2013).
- [10] Z. Xiaoming, W. Huizhen, W. Shuangjiang, Z. Yingying, C. Chunfeng, S. Jianxiao, Y. Zijian, D. Xiaoyang, D. Shurong, *J. Semicond.* **30**(3), 033001-1 (2009).
- [11] G. C. Yi, C. R. Wang, W. I. Park, *Semiconductor Science and Technology*, **20**(4), S22 (2005).
- [12] F. Tong, K. Kim, A. C. Ahyi, D.-J. Kim, Y. Wang, T. Smith, S. Lee, R. Thapa, E. Lim, J. Williams, Y. Sharma, K. K. Lee, H. Ahn, A. Modic, H. Park & M. Park, *International Scholarly Research Network ISRN Nanomaterials*, V. 2012, Article ID 651468.
- [13] Shabannia R. and Abu-Hassan, H., *Mater. Lett.* **90**, 156 (2013).
- [14] P. M. Aneesh, K.A. Vanaja, M.K. Jayaraj, Proc. SPIE 6639, *Nanophotonic Materials IV*, 66390J. (September 17, 2007).
- [15] N. Tang, J. Wang, H. Xu, H. Peng, C. Fan *Science in China E* **52**(8), 2200 (2009).
- [16] O. Lupon, V.M. Guerin, I.M. Tiginyanu, V.V. Ursaki, L. Chow, H. Heinrich, T. Pauporte, *J. Photochem. Photobiol. A Chem.* **211**, 65 (2010).
- [17] N.S. Kumar , K.V. Bangera, G.K. Shivakumar , *Appl. Nanosci.* **4**, 209 (2014).
- [18] A.M. Torres-Huerta, M. A. Dominguez-Crespo, S. B. Brachetti-Sibaja, J. Arenas-Alatorre, A. Rodriguez-Pulido, *Thin Solid Films* **519**(18), 6044 (2011).
- [19] B. D. Yao, Y. F. Chan, N. Wang, *Applied Physics Letters*, **81**(4), 757 (2002).
- [20] B. L. Zhu, X.Z.Zhao, F.H.SuetalVacuum **84**(11), 1280 (2010).
- [21] X.Pan, P.Ding, H.HeetalOptics Communications **285**(21-22), 4431 (2012).
- [22] WK Tan, KA Razak, K Ibrahim, Z Lockman, *J. Alloys Compd.* **509**, 820 (2010).
- [23]. S. Ezhilvalavan T.R.N. Kutty, *Mater. Chem. Phys.* **49**, 258 (1997).
- [24] G. Amin, M. H. Asif, A. Zainelabdin, S. Zaman, O. Nur, M. Willander, *Journal of Nanomaterials*, Vol. 9, 2011.
- [25] D. Polsongkram, P. Chamninok, S. Pukird, L. Chow, O. Lupon, G. Chai, *Physica B* **403**, 3713 (2008).
- [26] R. Shabannia, *Iran. J. Sci. Technol. Trans. Sci.* 2016.
- [27] A. F. Abdulrahman, S. M. Ahmed, N. M. Ahmed, M. A. Almessiere, *Digest Journal of Nanomaterials and Biostructures*, **11**(3), 1007 (2016).
- [28] A. F. Abdulrahman, S. M. Ahmed, N. M. Ahmed, M. A. Almessiere, *Digest Journal of Nanomaterials and Biostructures*, **11**(4), 1073 (2016).
- [29] Ahmed F., Abdulrahman, Sabah M., Ahmed, Naser M., Ahmed, *Science Journal of UOZ*, **5**(1), 128 (2017).
- [30] L. Roza, M. R., A. Umar, M. Salleh, *Journal of Alloys and Compounds*, 618, 153 (2015).
- [31] R. Shabannia, H. Abu Hassan, *Electron. Mater. Lett.* **10**(40), 837 (2014).

- [32] A., Sugianto, Irmansyah, Journal of Materials Physics and Chemistry, **2** (2), 34 (2014).
- [33] M. F. M., M.H. M., T. S., S. A., S. A., A. S. I., R. M. S., A. H. A., H. A. Khan & M. R. M. Japanese Journal of Applied Physics, **55**, 01AE15 (2016).
- [34] C. Ting, C. Li, C. Kuo, C. Hsu, H. Wang, M. H. Yang, Thin Solid Films, **518**, 4156 (2010).
- [35] M. T., N. M., D. Velauthapillai, C. Lee, Solar Energy **106**, 143 (2014).
- [36] A. Y., R. Sharma, O. Game, A. Banpurkar, Current Applied Physics, **11**, S113 (2011).
- [37] S.Q. Hussain, et al., Materials Science in Semiconductor Processing (2015), <http://dx.doi.org/10.1016/j.mssp.2015.02.024i>.
- [38] R. Idiawati, N. Mufti, A. Taufiq, H. Wisodo, I. K. R. Laila, Sunaryono, A. Fuad, IOP Conf. Series: Materials Science and Engineering, **202**, 012050 (2017).
- [39] R. N. Gayan, R. Bhar, A. K. Pal, Indian Journal of pure & Applied physics **48**, 385 (2010).
- [40] M. F. Malek, M. H. Mamat, M. Z. Sahdan, M. M. Zahidi, Z. Khusaimi, M. R. Mahmood, Thin Solid Films **527**, 102 (2013).
- [41] K. C. Yung, H. Liem, and H. S. Choy, J. Phys., D **42**, 185002 (2009).
- [42] C. V. Ramana, R. J. Smith, and O. M. Hussain, Phys. Status Solidi, A **199**, R4 (2003).
- [43] H. Lin, C. P. Huang, W. Li, C. Ni, S. I. Shah, and Y.-H. Tseng, Appl. Catal., B **68**, 1 (2006).
- [44] R. S. Yadav, P. Mishra, and A. C. Pandey, Ultrason. Sonochem. **15**, 863(2008).
- [45] Y.S. Kim, W.P. Tai, S.J. Shu, Thin Solid Films, **491**, 153 (2005).
- [46] S.H. Mohamed, A.M.A. El-Rahman, A.M. Salem, L. Pichon, F.M. El-Hossary, J. Phys. Chem. Solids, **67**, 2351(2006).
- [47] J. Tauc, R. Grigorovici, A. Vancu, Phys. Status Solidi B **15**, 627 (1966).
- [48] L. H, H. C, Li W, Ni C, Shah S and Tseng Y, Appl. Catal. B Environ., **68**(1–2), 1 (2006).
- [49] F.V. Molefe, L.F. Koao, J.J. Dolo, B.F. Dejene, Physica B, **439**, 185 (2014).
- [50] R. N. Gayen, R. Bhar & A. K. Pal, Indian Journal of Pure & Applied Physics, **48**, 385 (2010).
- [51] J.Y. Xing, Z.H. Xi, Q. X., X.D Z., & J.H. Song, Appl. Phys. Lett., **83**(9). 1689 (2003).
- [52] A. M. Holi, Z. Zainal, Z. A. Talib, H-N. Lim, C.-C. Yap, S-K. Chang, A. K. Ayal, Optik, **127**, 11111 (2016).
- [53] B.L. Zhu, X.H. Sun, S.S. Guo, X.Z. Zhao, J. Wu, R. Wu, J. Liu, Jpn. J. Appl. Phys. **45**, 7860 (2006).
- [54] M. Caglar, S. Illican, Y. Caglar, F. Yakuphanoglu, Appl. Surf. Sci. **255**, 4491 (2009).
- [55] Foo K L, Hashim U, Muhammad K and Voon C H, Nanoscale Res. Lett., **9** (1), 429 (2014).
- [56] P. S. Venkatesh, V. Ramakrishnan, K. Jeganathan, Physica B **481**, 204 (2016).
- [57] Ahmed F. Abdulrahman, Sabah M. Ahmed, Naser M. Ahmed and Munirah A Almessiere, AIP Conference Proceedings, **1875**, 020004 (2017); doi: 10.1063/1.4998358.
- [58] W.B. Mi, H.L. Bai, H. Liu, C.Q. Sun, J. Appl. Phys. **101**, 023904 (2007).
- [59] H.M. Zhong, J.B. Wang, X.S. Chen, Z.F. Li, W.L. Xu, W. Lu, J. Appl. Phys. **99**, 103905 (2006).
- [60] F. Decremps, J. Pellicer-Porres, A.M. Saitta, J.-C. Chervin, A. Polian, Phys. Rev. B, **65**, 092101 (2002).
- [61] N. I. Rusli, M. Tanikawa, M. R. Mahmood, K. Yasui, A. M. Hashim, Materials **5**, 2817 (2012).
- [62] W. K. Tan, K. Abdul Razak, Z. Lockman, G. Kawamura, H. Muto, A. Matsuda, Journal of Solid State Chemistry **211**, 146 (2014).